CMLS, Cell. Mol. Life Sci. 57 (2000) 1471–1481
1420-682X/00/101471-11 $ 1.50 + 0.20/0

CMLS Cellular and Molecular Life Sciences

Research Article

Oxidative stress and hypoxia-like injury cause Alzheimer-type molecular abnormalities in central nervous system neurons

S. M. de la Monte[a–c]*, T. R. Neely[a], J. Cannon[a] and J. R. Wands[a,c]

Departments of [a]Medicine, [b]Pathology, and [c]Pathobiology, Rhode Island Hospital, Brown University School of Medicine, 55 Claverick Street, Providence, Rhode Island 02903, USA, Fax + 1401 444 2939; e-mail: delamonte@hotmail.com

Received 24 May 2000; received after revision 7 July 2000; accepted 27 July 2000

Abstract. Neuronal loss and neuritic/cytoskeletal lesions (synaptic disconnection and proliferation of dystrophic neurites) represent major dementia-associated abnormalities in Alzheimer's disease (AD). This study examined the role of oxidative stress as a factor contributing to both the cell death and neuritic degeneration cascades in AD. Primary neuron cultures were treated with H_2O_2 (9–90 μM) or desferrioxamine (2–25 μM) for 24 h and then analyzed for viability, mitochondrial mass, mitochondrial function, and pro-apoptosis and sprouting gene expression. H_2O_2 treatment causes free-radical injury and desferrioxamine causes hypoxia-type injury without free radical generation. The H_2O_2-treated cells exhibited sustained viability but neurite retraction, impaired mitochondrial function, increased levels of the pro-apoptosis gene product CD95/Fas, reduced expression of N2J1-immunoreactive neuronal thread protein and synaptophysin, and reduced distribution of mitochondria in neuritic processes. Desferrioxamine treatment resulted in dose-dependent neuronal loss associated with impaired mitochondrial function, proliferation of neurites, and reduced expression of GAP-43, which has a role in path-finding during neurite outgrowth. The results suggest that oxidative stress can cause neurodegeneration associated with enhanced susceptibility to apoptosis due to activation of pro-apoptosis genes, neurite retraction (synaptic disconnection), and impaired transport of mitochondria to cell processes where they are likely required for synaptic function. In contrast, hypoxia-type injury causes neuronal loss with proliferation of neurites (sprouting), impaired mitochondrial function, and reduced expression of molecules required to form and maintain synaptic connections. Since similar abnormalities occur in AD, both oxidative stress and hypoxic injury can contribute to AD neurodegeneration.

Key words. Oxidative stress; mitochondria; neuritic sprouting; neurodegeneration.

Two of the major structural abnormalities that correlate with dementia in Alzheimer's Disease (AD) include increased cell death and cytoskeletal/neuritic pathology. Although cell death may be caused by more than one mechanism, several studies have demonstrated an important role for apoptosis mediated by enhanced sensitivity to oxidative stress [1–6] and constitutive activation of pro-apoptosis genes such as p53, CD95, and Bax [7–10]. In addition, impaired mitochondrial (mt) function due to oxidative stress, oxygen free radical damage, and accumulation of mtDNA mutations may induce or propagate aging-associated disease pro-

* Corresponding author.

cesses, including neurodegeneration [11]. mtDNA is not protected by histones or DNA-binding proteins, and in the central nervous system (CNS), mtDNA repair mechanisms have not yet been identified. mtDNA damage from continuous exposure to high levels of reactive oxygen species and free radicals is mediated by intra-mitochondrial accumulation of 8-oxo-7,8-dihydro-2′-deoxyguanosine (8-OH-dG) [11, 12]. 8-OH-dG is an abnormal nucleotide that accumulates in damaged mtDNA and causes base mispairing, random point mutations, and deletions [11, 12]. Importantly, damaged mitochondria can replicate because the enzymes required for mitochondrial replication are encoded by genomic DNA. Increased abundance of defective mtDNA that encodes respiratory enzymes can impair electron transport and enhance production of reactive oxygen species, furthering oxidative damage to mitochondria. This problem could be compounded by increased peroxidation of lipids and oxidative modification of proteins by reactive oxygen species and hydrogen peroxide (H_2O_2). Recently, we demonstrated increased mtDNA damage associated with increased 8-OH-dG immunoreactivity and reduced mitochondrial gene expression in AD [13], suggesting that environmental or systemic disease factors could contribute to the progression of AD neurodegeneration.

Little is known about the molecular pathogenesis of AD-associated cytoskeletal and neuritic pathology, including neurofibrillary tangles, dystrophic neurites, and neuropil threads. These lesions characteristically contain paired-helical filaments (PHFs) composed of insoluble fibrils generated from hyperphosphorylated tau, together with other cytoskeletal proteins and ubiquitin. tau phosphorylation can be induced by the activation of proline-directed protein kinases [14] including cyclin-dependent kinase 5 (cdk-5), glycogen synthase kinase-3β (GSK-3β), and Erk-mitogen-activated protein kinase (MAPK) [15–18]. cdk-5 is activated by its association with a brain-specific regulatory partner, p35 [19, 20], whereas GSK-3 and Erk-MAPK are ubiquitously expressed and activated by extracellular growth factors. Recent evidence suggests that tau hyperphosphorylation of tau and intraneuronal accumulations of fibrillar bundles resembling neurofibrillary tangles could be induced by constitutive over-expression of p25, a highly stable, catalytically active but truncated subunit of the p35 regulatory partner of cdk-5 [21]. Moreover, there is evidence that increased levels of cdk-5 can be associated with neuronal apoptosis [21–23]. In addition, we have obtained preliminary evidence that apoptosis caused by nitric oxide synthase 3 (NOS-3) over-expression or oxygen free radical injury is associated with increased neuronal levels of p25 [24].

One important additional clue concerning the pathogenesis of the cytoskeletal/neuritic pathology in AD is that the cortical neurites are immunoreactive with antibodies to several sprouting and growth-associated molecules including synaptophysin, the 43 to 46-kDa phosphoprotein, GAP-43, NOS-3, and neuronal thread protein (NTP). Since these same molecules are abundantly expressed during development and regeneration, the neuritic sprouting that occurs in AD could represent a growth response. Neuritic growth in the context of AD neurodegeneration could represent attempted regeneration of viable, healthy neurons following synaptic disconnection due to death of other neurons. Alternatively, the neuritic sprouting may correspond to a degenerative reaction in cells that are either intrinsically damaged, or injured by trophic factor withdrawal due to cell loss. If the neuritic sprouting in AD is indeed degenerative and therefore a form of 'sick sprouting,' it would constitute an additional mechanism of cell death. On the other hand, if the neuritic sprouting represents a healthy regenerative response, then therapeutic rescue should be directed toward bolstering the viability and function of this vulnerable population of neurons. Our hypothesis is that at least some aspects of the aberrant neuritic sprouting gene expression in AD represent a degenerative response in neurons that are destined to die. To test this hypothesis, we examined the levels of pro-apoptosis and sprouting-related molecules in CNS neuronal cells subjected to oxygen free radical or hypoxia-type injury.

Materials and methods

In vitro Model. Post-mitotic primary neuron (rCBN) cultures were generated with cerebellar cortical tissue from 6 to 7-day-old rat pups. The cultures were maintained in Dulbecco's modified Eagle's medium supplemented with 10% fetal calf serum, 2 mM glutamine, 10 mM non-essential amino acid mixture (Gibco-BRL, Grand Island, NY), 25 mM KCl, and 9 g/l glucose (complete neuronal medium) [25]. Proliferation of non-neuronal cells was inhibited by addition of cytosine arabinoside (6 μM) 24 h after seeding. To induce oxidative stress, cultures were treated with 9–90 μM H_2O_2 or 2.5–25 μM desferrioxamine mesylate for 24 h. H_2O_2 causes oxidative stress and potentially oxygen free radical injury. Desferrioxamine mesylate is a chelator of ferric iron that inhibits the formation of free radicals [26] but simulates an experimental model of hypoxia-induced injury [27]. The cultures were analyzed for viability, mitochondrial mass, mitochondrial function, and expression of the CD95 pro-apoptosis gene, and the GAP-43, synaptophysin, and NTP sprouting-associated molecules. Assays were performed using cells seeded in 96-well plates, 6-well plates, or 10-cm^2 petri dishes. The 96-well micro-cultures permitted simultaneous analysis of 8–24 replicate culture wells. All studies were repeated at least three times.

Viability assays. Viability was measured by the crystal violet [28] assay which was performed with cells seeded into 96-well plates at a density of 2×10^4 cells/well. The absorbances were measured using a Spectracount plate reader (Packard, Meriden, Conn.). The crystal violet absorbance values increased linearly with cell density between 10^4 and 5×10^5 cells/well.

The microtiter immunocytochemical ELISA (MICE) assay of protein expression. The MICE assay is a rapid and sensitive method for quantifying immunoreactivity in micro (96-well)-cultures [29]. It was used to measure cellular expression of CD95, mitochondrial protein, cytochrome oxidase, GAP-43, synaptophysin, and NTP. NTP was detected using the N2J1 monoclonal antibody [30] that binds to the ~21-kDa form of NTP which increases in expression during experimental neuritic sprouting [31, 32] and AD neurodegeneration [30, 33]. The cells were fixed in Histochoice (Amresco, Solon, Ohio), permeabilized with 0.05% saponin in Tris-buffered saline (TBS; 50 mM Tris, pH 7.5, 0.9% NaCl), and blocked with Superblock-TBS (Pierce, Rockford, Ill.). The cells were then incubated overnight at 4 °C with primary antibody diluted in TBST-BSA. Immunoreactivity was detected using horseradish peroxidase-conjugated secondary antibody (Pierce) and the TMB-soluble peroxidase substrate (Pierce). Absorbances were measured at 450 nm using a Spectracount plate reader. To compare the levels of protein expression, corrections were made for differences in cell density. After measuring immunoreactivity, the plates were washed in TBS and the cells were stained with 0.1% Coomassie blue dye in 40% methanol/10% acetic acid. After extensively washing the plates in water, the dye was eluted with 1% SDS in PBS (200 µl/well). The absorbances (560 nm) were measured using a Spectracount plate reader (Packard, Meriden, Conn.). The MICE index was calculated from the ratio of the absorbances measured for immunoreactivity and cell density. Coomassie blue absorbance increases linearly with cell density between 1×10^4 and 5×10^5 cells per well. Eight or 24 replicate culture wells were analyzed in each experiment. All experiments were repeated at least three times.

Mitochondria labeling studies. Mitochondrial mass and function were evaluated using MitoTracker mitochondria-specific cell-permeable dyes (Molecular Probes, Eugene, Ore.). MitoTracker Green FM labels mitochondria irrespective of oxidative activity and is therefore used to assess mitochondrial mass. MitoTracker Red (CM-H_2Xros) accumulates only in metabolically active mitochondria and the reduced dihydrotetramethylrosamine is rendered fluorescent via oxidation within the mitochondria. Cells grown in 96-well plates were incubated with MitoTracker Red or MitoTracker Green FM for 15 min according to the manufacturer's instructions. The cells were rinsed in TBS and fluorescence light units were measured with a Fluorocount plate reader (Packard). Subsequently, cells were stained with H33258 to determine cell density using the Fluorocount plate reader. H33258 fluorescence intensity increases linearly with cell number between 1×10^4 and 5×10^5 cells per well (data not shown). MitoTracker Red/H33258 and MitoTracker Green/H33258 ratios were used as indices of mitochondrial function and mitochondrial mass, respectively.

Results

Effects of H_2O_2 or desferrioxamine treatment on rCBN culture viability.. H_2O_2 treatment was associated with minimal reductions in viability, except at the highest concentration (90 µM), which caused an ~42% cell loss in the cultures (fig. 1A). In contrast, desferrioxamine treatment resulted in concentration-dependent reductions in viability (fig. 1B). Therefore, the oxidative stress and possible oxygen free radical injury did not kill the neuronal cells, whereas the hypoxia-like injury in the absence of free radical damage did cause neuronal cell death.

Effects of H_2O_2 or desferrioxamine treatment on CD95 (Apo-1/Fas receptor) expression in rCBN cultures. CD95 is one of the pro-apoptosis molecules expressed at increased levels in brains with AD and other forms of neurodegeneration [7, 8]. Cells treated with 18 µM or higher concentrations of H_2O_2 exhibited sharply increased (five- or sixfold) levels of CD95 expression (fig. 2A). In contrast, desferrioxamine treatment had little effect on CD95 expression except at the highest concentration used (25 µM) (fig. 2B). This suggests that CD95 expression in CNS neurons correlates more with oxidative stress than with hypoxia-induced injury or death of CNS neurons. Moreover, these observations suggest that increased expression of CD95 is not sufficient to cause apoptosis in neurons, although it may render them more susceptible to other pro-apoptosis stimuli.

Effects of H_2O_2 or desferrioxamine treatment on mitochondrial protein and cytochrome oxidase expression. To determine the potential effect of oxidative stress-induced injury versus hypoxia-like injury on mitochondrial mass and mitochondrial function, we assessed mitochondrial protein and cytochrome oxidase (COX) expression in H_2O_2- and desferrioxamine-treated rCBN cells. Mitochondrial protein was detected with a monoclonal antibody generated to mitochondria (Chemicon Temecula, Calif.). This anti-mitochondrial antibody immunoreacts with an uncharacterized ~65-kDa protein by Western blot analysis, and exhibits a beaded or granular profile that is typical of mitochondria and identical to the labeling patterns observed with anti-

COX by immunocytochemical staining (data not shown). Monoclonal antibodies to COX, complex IV (Molecular Probes, Eugene, Ore.) detected the expected ~35-kDa band by Western blot analysis (data not shown). Using the MICE assay, we observed H_2O_2 and desferrioxamine concentration-dependent reductions in COX expression (fig. 3A, C), but no change in the levels of mitochondrial protein (fig. 3B, D). This suggests that both H_2O_2 and desferrioxamine neurotoxicity impair mitochondrial function yet have little or no effect on mitochondrial mass.

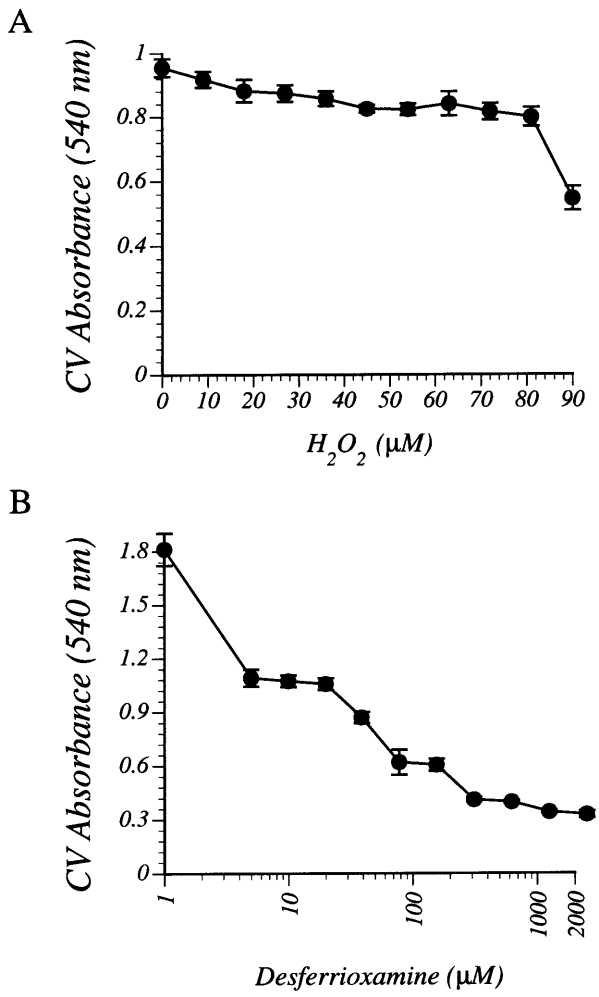

Figure 1. Effects of H_2O_2 (*A*) or desferrioxamine (*B*) treatment on neuronal viability. Primary post-mitotic neuron cultures generated from rat cerebellar granule cells were seeded in 96-well plates (2×10^4 cells/well) and treated with 0–90 μM H_2O_2 or 0–25 μM desferrioxamine for 24 h, after which viability was measured using the crystal violet (CV) assay. Absorbances were measured at 540 nm using an automated ELISA plate reader. The graphs depict mean and standard deviations obtained for eight replicate culture wells. Identical results were obtained in three separate experiments.

MitoTracker detection of reduced mitochondrial function following H_2O_2 or desferrioxamine treatment. Mitochondrial function and mitochondrial mass were further

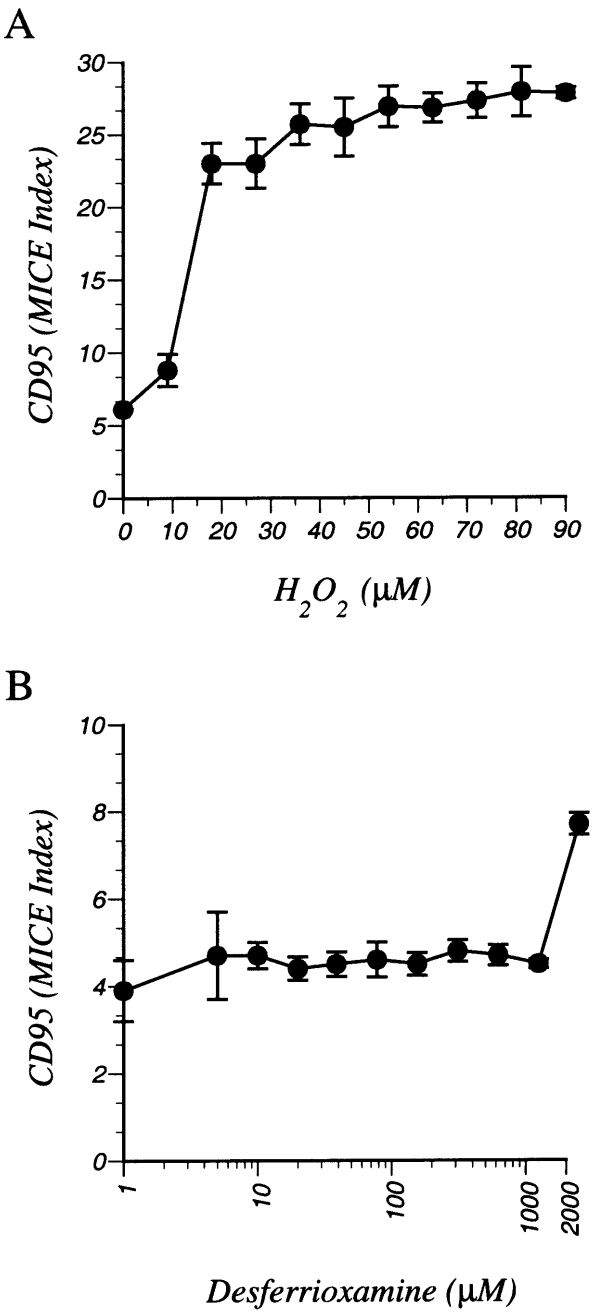

Figure 2. Effects of H_2O_2 (*A*) or desferrioxamine (*B*) treatment on CD95 Fas receptor expression. Primary post-mitotic neuron cultures generated from rat cerebellar granule cells were seeded in 96-well plates (2×10^4 cells/well) and treated with 0–90 μM H_2O_2 or 0–25 μM desferrioxamine for 24 h. Immunoreactivity was measured by the microtiter immunocytochemical ELISA (MICE) assay (see Materials and methods). The MICE index refers to immunoreactivity corrected for cell density. The graphs depict mean and standard deviations obtained for eight replicate culture wells. Identical results were obtained in three separate experiments.

evaluated using the MitoTracker mitochondria-specific cell-permeable dyes. MitoTracker Red accumulates only in metabolically active mitochondria and the reduced dihydrotetramethyl rosamine is rendered fluorescent via oxidation within mitochondria. MitoTracker Green labels mitochondria irrespective of oxidative activity and the dye is therefore used to assess mitochondrial mass. Fluorescence intensity was measured in a microplate reader. Cell density was measured by subsequently staining the cells with Hoechst H33258. H33258 fluorescence increases linearly with cell number between 1×10^4 and 5×10^5 cells per well (data not shown). Both the H_2O_2- and desferrioxamine-treated rCBN cultures exhibited concentration-dependent reductions in the MitoTracker Red/H33258 ratios (fig. 4A, C). In contrast, the same treatments caused minimal alterations in the levels of MitoTracker Green fluorescence (fig. 4B, D). However, in cultures treated with moderately high concentrations of H_2O_2 or desferrioxamine, the levels of MitoTracker Green fluorescence

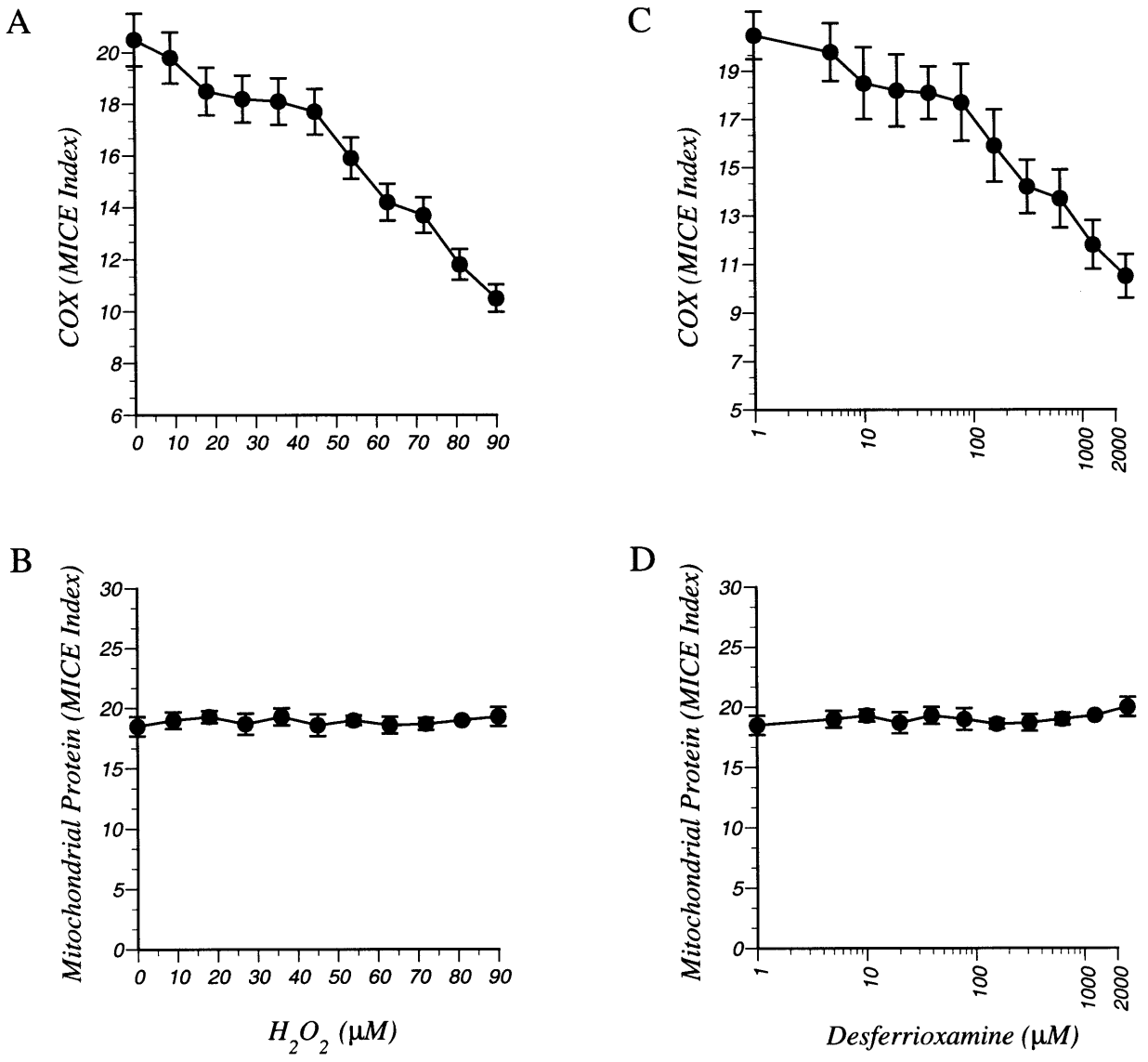

Figure 3. Effects of H_2O_2 (*A*, *B*) or desferrioxamine (*C*, *D*) treatment on cytochrome oxidase (COX) and mitochondrial protein expression. COX expression was used as a measure of mitochondrial function, and mitochondrial protein as a measure of mitochondrial mass. Primary post-mitotic neuron cultures generated from rat cerebellar granule cells were seeded in 96-well plates (2×10^4 cells/well) and treated with 0–90 μM H_2O_2 or 0–25 μM desferrioxamine for 24 h. Immunoreactivity was measured by the MICE assay (see Materials and methods). The MICE index refers to immunoreactivity corrected for cell density. The graphs depict mean and standard deviations obtained for eight replicate culture wells. Identical results were obtained in three separate experiments.

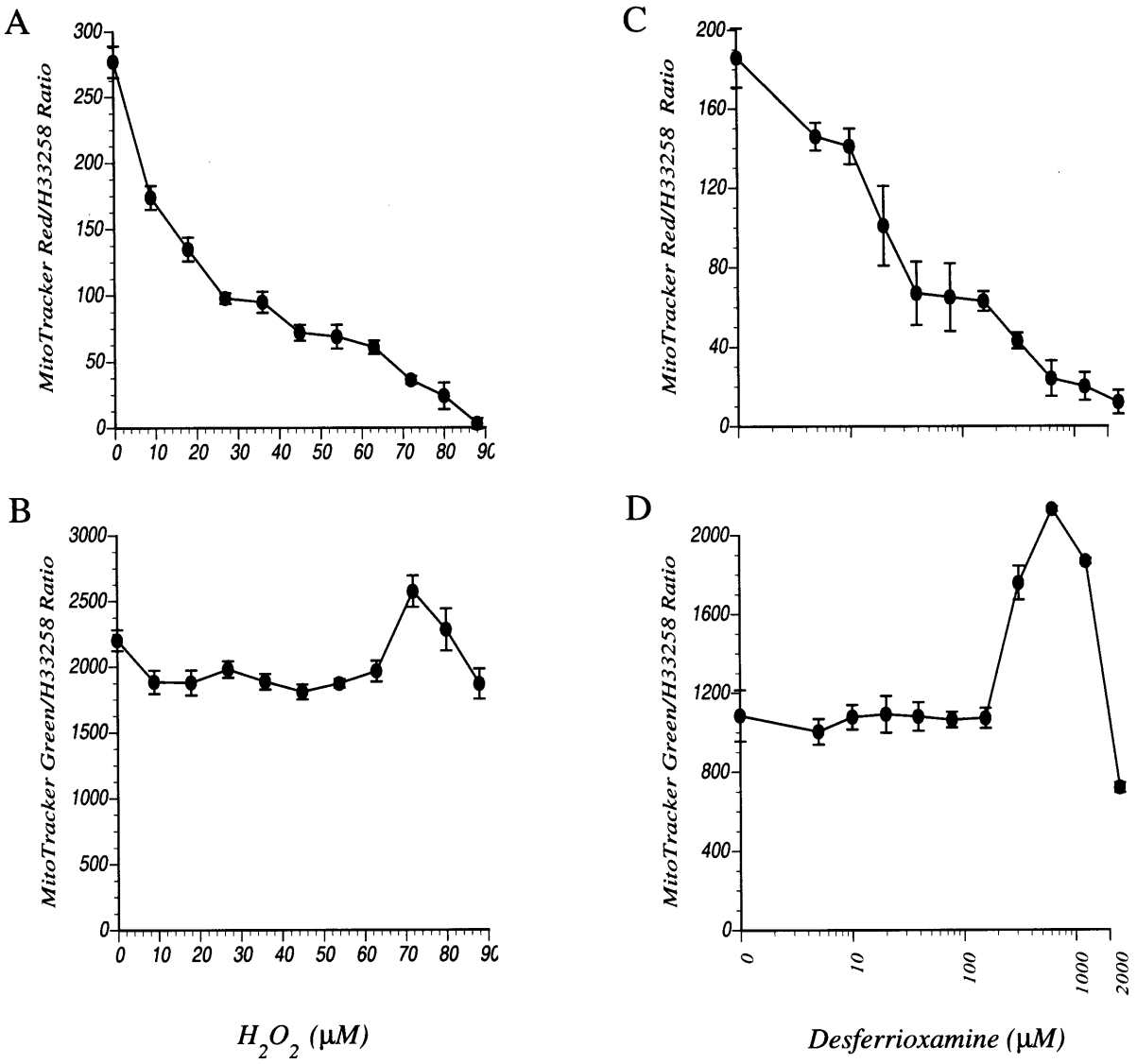

Figure 4. Effects of H_2O_2 (*A*, *B*) or desferrioxamine (*C*, *D*) treatment on MitoTracker Red (*A*, *C*) and MitoTracker Green (*B*, *D*) fluorescence labeling. MitoTracker Red fluorescence corresponds to functional mitochondria, whereas MitoTracker Green fluorescence corresponds to mitochondrial mass. Primary post-mitotic neuron cultures were seeded in 96-well plates (2×10^4 cells/well) and treated with 0–90 μM H_2O_2 or 0–25 μM desferrioxamine for 24 h. The cells were then labeled for 15 min with MitoTracker Red or Green dye, and fluorescence intensity was measured using an automated microplate fluorometer (Fluorocount). The MitoTracker light unit values were corrected for cell density by subsequently labeling the cells with Hoechst H33258 and measuring the fluorescence intensities. H33258 fluorescence increases linearly with cell density between 10^4 and 5×10^5 cells/well. The graphs depict the means and standard deviations of the MitoTracker/H33258 ratios.

were conspicuously increased, suggesting that mitochondria may have proliferated in response to those degrees of oxidative stress. The MitoTracker labeling results correspond with the MICE assay measurements of COX and mitochondrial protein expression and indicate that both oxygen free radical injury and hypoxia-like insults impair mitochondrial function without depleting mitochondria.

In situ analysis of MitoTracker Green fluorescence labeling. To determine the effect of H_2O_2 or desferrioxamine exposure on the distribution of mitochondria, MitoTracker-labeled cells were examined by fluorescence microscopy. Control cells exhibited uniformly bright MitoTracker Red and Green fluorescence with prominent labeling of both the cell bodies and neuritic processes (figs 5A, 6A). Following H_2O_2 or desferrioxamine

treatment, MitoTracker Red fluorescence was sharply reduced and scarcely detectable in the cells (data not shown), corresponding with the quantitative assessments of the labeling indices as shown in figure 4. However, with increasing concentrations of H_2O_2 up to 45 μM, MitoTracker Green labeling was primarily reduced in the neuritic processes (fig. 5B, C), whereas at higher concentrations, labeling was markedly reduced in both the cell bodies and neurites (fig. 5D). With increasing concentrations of desferrioxamine, the cultures exhibited markedly increased densities of MitoTracker Green-labeled neuritic processes (fig. 6B, C), despite virtually undetectable MitoTracker Red fluorescence labeling. At high concentrations of desferrioxamine (> 7.5 μM), the remaining cells still had detectable MitoTracker Green fluorescence labeling of both cell processes and cell bodies (fig. 6D).

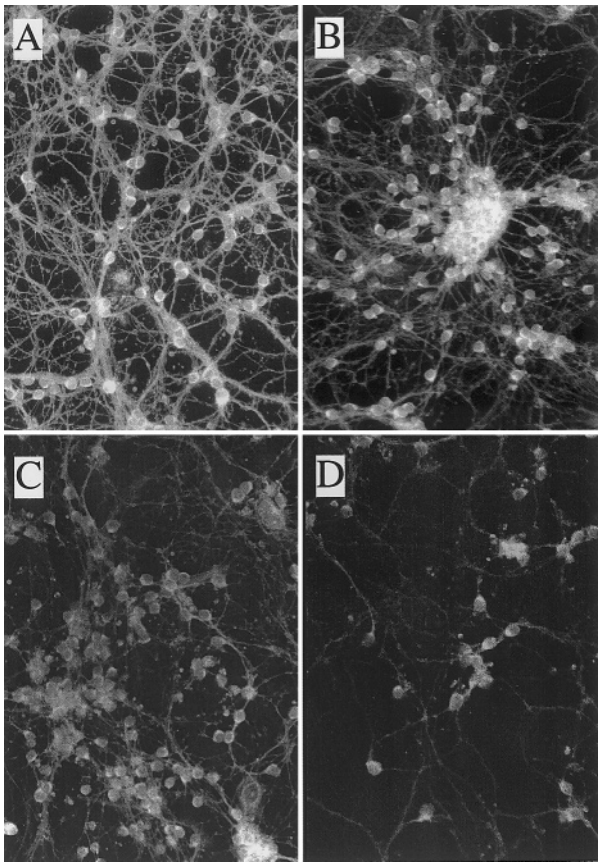

Figure 5. Effects of H_2O_2 treatment on the cellular distribution of MitoTracker Green fluorescence. Primary post-mitotic neuron cultures were seeded in 96-well plates (2×10^4 cells/well) and treated with nothing (*A*), 18 μM (*B*), 45 μM (*C*), or 90 μM (*D*) H_2O_2 for 24 h. The cells were labeled for 15 min with MitoTracker Green dye and examined using a fluorescence microscope.

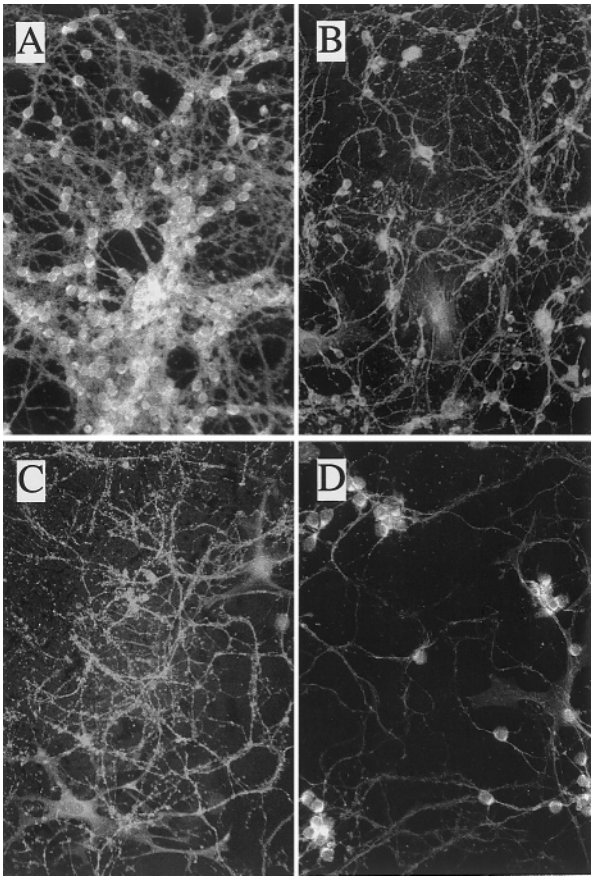

Figure 6. Effects of desferrioxamine treatment on the cellular distribution of MitoTracker Green fluorescence. Primary post-mitotic neuron cultures were seeded in 96-well plates (2×10^4 cells/well) and treated with nothing (*A*), 5 μM (*B*), 10 μM (*C*), or 15 μM desferrioxamine for 24 h. The cells were labeled for 15 min with MitoTracker Green dye and examined using a fluorescence microscope.

Neuronal growth and sprouting gene expression. To determine the effects of oxidative stress and hypoxia-type injury on the expression of neuritic sprouting-associated proteins, we used the MICE assay to measure GAP-43, NTP, and synaptophysin immunoreactivity in cells treated with H_2O_2 or desferrioxamine (fig. 7). Note that the immunoreactivity measured by the MICE assay is corrected for differences in cell density [29]. Cells treated with 9–90 μM H_2O_2 exhibited control levels of GAP-43 expression, and dose-dependent reductions in N2J1-immunoreactive NTP, and synaptophysin (fig. 7A–C). Cells treated with 2.5–25 μM desferrioxamine exhibited marked concentration-dependent reductions ($\sim 50\%$) in GAP-43 expression and moderate reductions (25–35%) in the levels of N2J1-immunoreactive NTP, and synaptophysin (fig. 7D–F). The N2J1

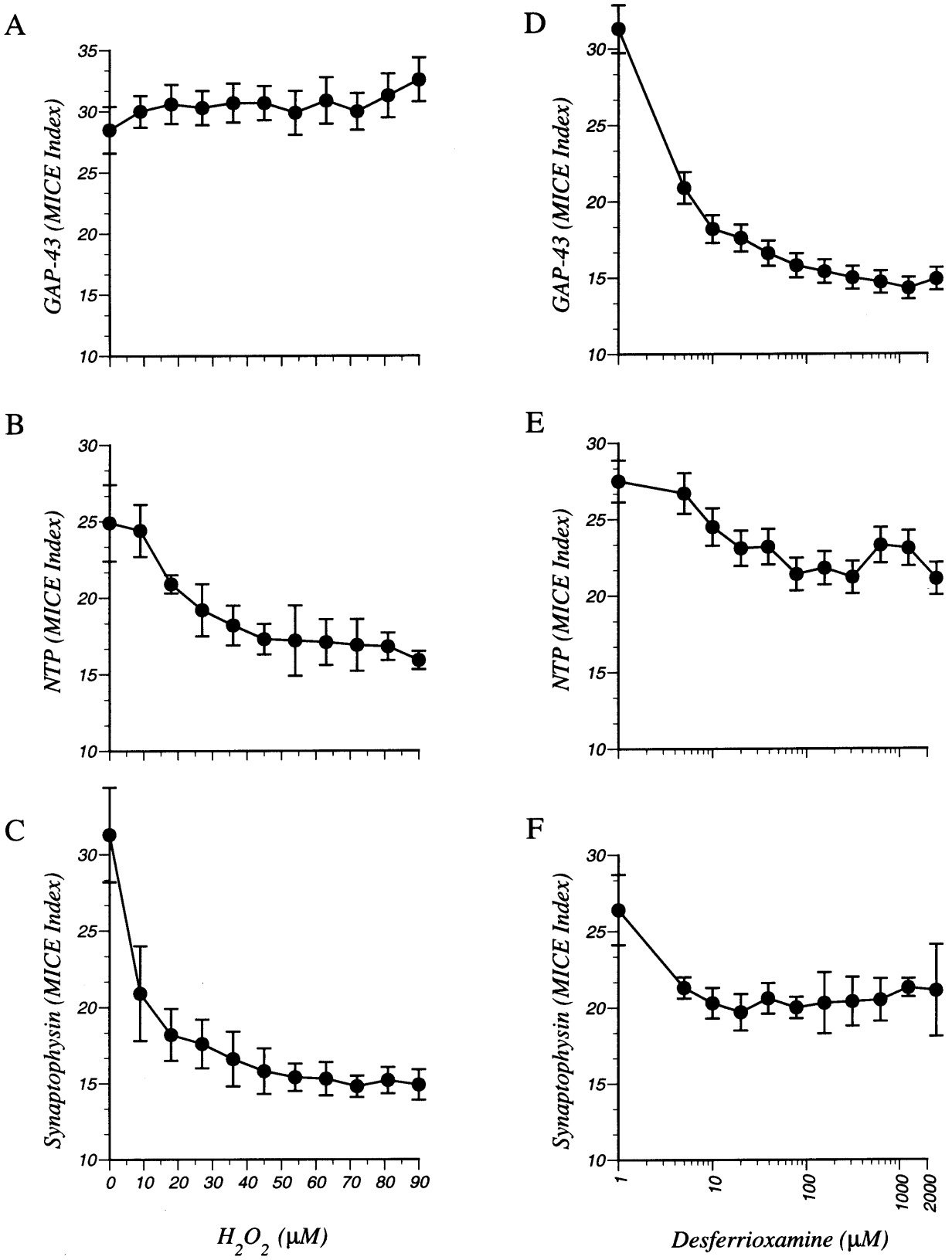

Figure 7. Modulation of sprouting gene expression with H_2O_2 (*A–C*) or desferrioxamine (*D–F*) treatment. GAP-43 (*A*, *D*), N2J1-immunoreactive NTP (*B*, *E*), and synaptophysin (*C*, *F*) immunoreactivity were measured using the MICE assay. The MICE indices represent levels of immunoreactivity corrected for cell density (see Materials and methods). Graphs depict mean and standard deviation of immunoreactivity levels detected in 24-replicate culture wells. All experiments were repeated at least three times with similar results.

monoclonal antibody detects the ~21-kDa NTP species that increases with experimental neuritic sprouting, hypoxic-ischemic injury, and AD neurodegeneration [30–33].

Discussion

This study demonstrated that H_2O_2 treatment of CNS neuronal cultures resulted in increased expression of the CD95 pro-apoptosis gene and impaired mitochondrial function manifested by sharply reduced levels of COX and MitoTracker Red fluorescence. In addition, oxidative stress inhibited the expression of N2J1-immunoreactive NTP and synaptophysin, but had little or no effect on culture viability (cell density), mitochondrial mass, or GAP-43 expression. In contrast, desferrioxamine treatment caused neuronal death associated with markedly reduced levels of COX expression and MitoTracker Red fluorescence. In addition, desferrioxamine treatment resulted in sharply reduced (by ~50%) levels of GAP-43, and modest inhibition (20–30%) of N2J1-immunoreactive NTP and synaptophysin expression. H_2O_2 exposure causes oxidative stress and can lead to free radical injury by promoting hydroxyl radical production. Therefore, H_2O_2 exposure can damage DNA either directly or through apoptosis mechanisms. Desferrioxamine is a chelator of ferric iron and an inhibitor of both ATP synthesis and free radical generation. Desferrioxamine treatment is used as a pharmacological model of hypoxic injury. Therefore, this study compared neuronal responses to oxidative stress and hypoxia-like injury in CNS neurons because either type of environmental stress could potentially precipitate or exacerbate the course of AD neurodegeneration.

In AD, neuronal loss has been linked to increased levels of pro-apoptosis gene products such as p53, CD95 [7, 8], and Bax [9, 34–36] and increased activation of CPP32 caspase [36, 37], suggesting that the apoptosis of cortical neurons is due to heightened sensitivity to oxygen free radial injury [6]. The finding that H_2O_2 treatment increased the expression of CD95 but did not cause cell death suggests that apoptosis is not a necessary outcome of oxidative stress in CNS neurons. Although the H_2O_2-treated cells remained viable, they were probably rendered more susceptible to further oxidative stress because increased levels of CD95 can precipitate caspase-mediated cell death. The effects of desferrioxamine toxicity on neuronal viability and function reflect the cellular responses to hypoxia in the absence of free radical injury. The concentration-dependent reductions in neuronal viability were not associated with increased levels of CD95 expression. This suggests that activation of the CD95 gene, and perhaps other pro-apoptosis genes, in AD is the result of free radical injury to neurons.

Both the H_2O_2 and desferrioxamine treatments were associated with dose-dependent reductions in COX immunoreactivity and MitoTracker Red fluorescence, whereas mitochondrial protein expression and MitoTracker Green fluorescence were not inhibited. These findings indicate that oxidative stress and hypoxia-like injury can cause substantial impairment of mitochondrial function with little effect on mitochondrial mass or abundance. In other words, oxidative stress and hypoxic injury result in the accumulation of defective mitochondria in neurons. Recent studies suggest that oxidative stress caused by hydrogen peroxide exposure can result in down-regulation of mitochondrial RNA expression and calcium-dependent RNA degradation [38–40]. Therefore, in neuronal cells, oxidative stress-induced impairment of mitochondrial function and reduction in mitochondrial enzyme expression may be mediated by selective degradation of mitochondrial RNA. If the affected cells do not die by necrosis or apoptosis, they may remain functionally impaired due to the accumulation of defective mitochondria. Increased densities of 'useless' cells may interfere with normal remodeling processes in the brain. On the other had, injured but marginally viable neurons with compromised mitochondrial function may be more susceptible to apoptosis, such that additional oxygen free radical or hypoxic injury could deplete the population of neurons that could be rescued therapeutically.

The fluorescence microscopy studies confirmed the global reductions in MitoTracker Red fluorescence detected with quantitative assays but, more important, demonstrated that the H_2O_2 treatment resulted in selectively reduced levels of MitoTracker Green labeling in the neuritic processes compared with the neuronal cell bodies. In contrast, the cell loss caused by desferrioxamine treatment resulted in an apparent proliferation of neuritic processes that were labeled with the MitoTracker Green dye. Since MitoTracker Red fluorescence reflects functional mitochondria, the persistent MitoTracker Green labeling in neurons subjected to oxidative stress or hypoxia-like injury reflected the distribution and abundance of mitochondria that were essentially non-functional. Therefore, although the H_2O_2-treated neurons remained 'viable' they were functionally impaired. Moreover, the reduced mitochondrial mass observed in neuritic processes of H_2O_2-treated cells suggests that oxidative stress-induced injury can promote neurodegeneration by inhibiting the transport of mitochondria to neuronal cell processes where they are required to maintain synaptic function. At the same time, the increased density of MitoTracker Green-labeled neurites in desferrioxamine-treated cultures that had very low levels of MitoTracker Red fluorescence suggests that the hypoxia-like injury can promote neuritic sprouting (?regenerative), but the proliferated neu-

rites may not be capable of forming or maintaining sound synaptic connections due to impaired mitochondrial function.

GAP-43 is a membrane-associated phosphoprotein localized in axons, neuritic processes, and the filpodia and lamellipodia of growth cones. GAP-43 has a role in axonal path-finding, neurite outgrowth, and regulating cytoskeletal organization in nerve endings [41]. Synaptophysin is a synaptic protein and marker of vesicular transport that may function in exocytosis and has an important role in the formation and maintenance of synapses. NTPs are a relatively novel family of molecules that are abundantly expressed in CNS neurons during development, neuritic sprouting, and following hypoxic-ischemic injury [31–33]. The N2J1 antibody detects the ~21-kDa NTP molecule that increase in expression during sprouting and with AD neurodegeneration [30, 32]. GAP-43, synaptophysin, and NTP immunoreactivities are increased in the cortical dystrophic neurites in brains with AD [33, 42–44]. Therefore, it was of interest to determine the extents to which oxidative stress and hypoxia-like injury modulated the expression of these sprouting-associated proteins.

The viable but injured H_2O_2-treated neuronal cells had sharply reduced expression of both NTP and synaptophysin, but control levels of GAP-43. Both N2J1-NTP and synaptophysin immunoreactivity are distributed predominantly in neurites and growth cones, whereas GAP-43 immunoreactivity is abundantly distributed in the neuronal perikarya and neurites. Therefore, the failure of mitochondria to be distributed in neuritic processes of H_2O_2-treated cells correlates with the reduced levels of N2J2-NTP and synaptophysin. The reductions in neuritic MitoTracker Green fluorescence occurred even at concentrations of H_2O_2 that do not result in neurite retraction (fig. 6B), suggesting that one consequence of oxidative stress is impairment of the transport of mitochondria to neurites and growth cones required to maintain synaptic integrity. Therefore, in AD, oxidative stress-mediated injury could exacerbate synaptic disconnection by impairing transport of mitochondria to growth cones and causing cytoskeletal collapse (neurite retraction).

Desferrioxamine treatment serves as a pharmacological model of hypoxia without free radical injury. Desferrioxamine treatment resulted in markedly reduced levels of GAP-43 (~ 50%) and moderately reduced levels of N2J1-NTP and synaptophysin (~ 20–30%) expression. These reductions in sprouting-associated genes occurred in the context of conspicuous cell loss, abundant proliferation of neurites, and marked impairment of mitochondrial oxidative function as manifested by the sharply reduced levels of MitoTracker Red fluorescence and COX expression. Since (presumably non-functioning) mitochondria were still abundantly distributed within neuritic processes, hypoxic injury unrelated to free radical generation may not impair mitochondrial transport, cytoskeletal function, or growth/sprouting mechanisms. However, neurons injured by hypoxia are still likely to be functionally impaired and unable to meet the energy demands for the synthesis of proteins required for neurite path-finding and maintenance of synaptic connections.

In summary, this study demonstrated that both oxidative stress and hypoxia-type injury substantially impair mitochondrial function but cause different types of neurodegeneration. Oxidative stress-induced neurodegeneration was associated with activation of pro-apoptosis genes, neurite retraction, and inhibition of synaptic and sprouting genes, whereas hypoxia-like injury resulted in neuronal cell death, prominent neuritic sprouting, and inhibition of GAP-43, NTP, and synaptophysin expression. Therefore, with respect to AD neurodegeneration, oxidative stress-induced injury could account for some aspects of synaptic disconnection and the increased susceptibility to apoptosis, whereas hypoxia-like injury could contribute to cell loss, synaptic disconnection, and the proliferation of cortical neurites. Moreover, the findings reported here suggest that: (i) CNS neurons injured by oxygen free radicals or hypoxia may be physically present but non-functional due to impaired energy metabolism; (ii) sprouting gene expression can persist in 'sick' neurons; (iii) impaired mitochondrial transport may contribute to synaptic disconnection, and (iv) the proliferation of neurites could represent a pathological response in cells that are not capable of generating sound synaptic connections due to impaired energy metabolism. Important for future studies will be to determine the extent to which these abnormalities in neuronal function are reversible.

Acknowledgements. This work was supported by grants AA-02666 and AA-10102 from the National Institutes of Health, and a grant from NYMOX Corporation.

1 Smith M. A., Hirai K., Hsiao K., Pappolla M. A., Harris P. L., Siedlak S. L. et al. (1998) Amyloid-beta deposition in Alzheimer transgenic mice is associated with oxidative stress. J. Neurochem. **70:** 2212–2215

2 Smith M. A., Sayre L. M., Anderson V. E., Harris P. L., Beal M. F., Kowall N. et al. (1998) Cytochemical demonstration of oxidative damage in Alzheimer disease by immunochemical enhancement of the carbonyl reaction with 2,4-dinitrophenylhydrazine. J. Histochem. Cytochem. **46:** 731–765

3 Yan S. D., Yan S.F., Chen X., Fu J., Chen M., Kuppusamy P. et al. (1995) Non-enzymatically glycated tau in Alzheimer's disease induces neuronal oxidant stress resulting in cytokine gene expression and release of amyloid beta-peptide. Nat. Med. **1:** 693–699

4 Sayre L. M., Zagorski M. G., Surewicz W. K., Krafft G. A. and Perry G. (1997) Mechanisms of neurotoxicity associated with amyloid beta deposition and the role of free radicals in

the pathogenesis of Alzheimer's disease: a critical appraisal. Chem. Res. Toxicol. **10:** 518–526
5 Smith M. A. and Perry G. (1995) Free radical damage, iron, and Alzheimer's disease. J. Neurol. Sci. Suppl. **134:** 92–94
6 Stadelmann C., Bruck W., Bancher C., Jellinger K. and Lassmann H. (1998) Alzheimer disease: DNA fragmentation indicates increased neuronal vulnerability, but not apoptosis. J. Neuropathol. Exp. Neurol. **57:** 456–464
7 Monte S. M. de la, Sohn Y. K. and Wands J. R. (1997) Correlates of p53- and Fas (CD95)-mediated apoptosis in Alzheimer's disease. J. Neurol. Sci. **152:** 73–83
8 Monte S. M. de la, Sohn Y. K., Ganju N. and Wands J. R. (1998) P53- and CD95-associated apoptosis in neurodegenerative diseases. Lab. Invest. **78:** 401–411
9 Su J. H., Deng G. and Cotman C. W. (1997) Bax protein expression is increased in Alzheimer's brain: correlations with DNA damage, Bcl-2 expression, and brain pathology. J. Neuropathol. Exp. Neurol. **56:** 86–93
10 Erro E. and Tunon T. (1997) Preliminary results of the study of neuronal death and the expression of bcl-2 protein in Alzheimer's disease. Rev. Med. Univ. Navarra **41:** 28–33
11 Richter C. (1992) Reactive oxygen and DNA damage in mitochondria. Mutat. Res. **275:** 249–255
12 Richter C. (1995) Oxidative damage to mitochondrial DNA and its relationship to ageing. Int. J. Biochem. Cell. Biol. **27:** 647–653
13 Monte S. M. de la, Robinson D., Cannon J. L., Neely T. R. and Wands J. R. (in press) Mitochondrial DNA damage as a mechanism of cell loss in Alzheimer's disease. Lab. Invest.
14 Mandelkow E. M. and Mandelkow E. (1993) Tau as a marker for Alzheimer's disease. Trends Biochem. Sci. **18:** 480–483
15 Sengupta A., Wu Q., Grundke-Iqbal I., Iqbal K. and Singh T. J. (1997) Potentiation of GSK-3-catalyzed Alzheimer-like phosphorylation of human tau by cdk5. Mol. Cell. Biochem. **167:** 99–105
16 Lovestone S., Reynolds C. H., Latimer D., Davis D. R., Anderton B. H., Gallo J. M. et al. (1994) Alzheimer's disease-like phosphorylation of the microtubule-associated protein tau by glycogen synthase kinase-3 in transfected mammalian cells. Curr. Biol. **4:** 1077–1086
17 Baumann K., Mandelkow E. M., Biernat J., Piwnica-Worms H. and Mandelkow E. (1993) Abnormal Alzheimer-like phosphorylation of tau-protein by cyclin-dependent kinases cdk2 and cdk5. FEBS Lett. **336:** 417–424
18 Hosoi T., Uchiyama M., Okumura E., Saito T., Ishiguro K., Uchida T. et al. (1995) Evidence for cdk5 as a major activity phosphorylating tau protein in porcine brain extract. J. Biochem. (Tokyo) **117:** 741–749
19 Tsai L. H., Delalle I., Caviness V. S. J.r, Chae T. and Harlow E. (1994) p35 is a neural-specific regulatory subunit of cyclin-dependent kinase 5. Nature **371:** 419–423
20 Ishiguro K., Kobayashi S., Omori A., Takamatsu M., Yonekura S., Anzai K. et al. (1994) Identification of the 23 kDa subunit of tau protein kinase II as a putative activator of cdk5 in bovine brain. FEBS Lett. **342:** 203–208
21 Patrick G. N., Zukerberg L., Nikolic M., Monte S. de la, Dikkes P. and Tsai L. H. (1999) Conversion of p35 to p25 deregulates Cdk5 activity and promotes neurodegeneration [see comments]. Nature **402:** 615–622
22 Honma N., Hosono Y., Kishimoto T. and Hisanaga S. (1997) Phosphorylation of retinoblastoma protein at apoptotic cell death in rat neuroblastoma B50 cells. Neurosci. Lett. **235:** 45–48
23 Ahuja H. S., Zhu Y. and Zakeri Z. (1997) Association of cyclin-dependent kinase 5 and its activator p35 with apoptotic cell death. Dev. Genet. **21:** 258–267
24 Monte S. M. de la, Ganju N., Luong T., Janssens S., Bloch K. D., Feroz N. et al. (1999) Over-expression of nitric oxide synthase-3 and free radical injury cause apoptosis and phsopho-tau accumulation in neuronal cells (abstract). J. Neuropathol. Exp. Neurol. **58:** 512
25 Nikolic M., Dudek H., Kwon Y. T., Ramos Y. F. and Tsai L. H. (1996) The cdk5/p35 kinase is essential for neurite outgrowth during neuronal differentiation. Genes Dev. **10:** 816–825
26 Zweier J. L., Kuppusamy P., Thompson-Gorman S., Klunk D. and Lutty G.A. (1994) Measurement and characterization of free radical generation in reoxygenated human endothelial cells. Am. J. Physiol. **266:** C700–C708
27 Gleadle J. M., Ebert B. L., Firth J. D. and Ratcliffe P. J. (1995) Regulation of angiogenic growth factor expression by hypoxia, transition metals, and chelating agents. Am. J. Physiol. **268:** C1362–C1368
28 Clement M. V. and Stamenkovic I. (1996) Superoxide anion is a natural inhibitor of FAS-mediated cell death. EMBO J **15:** 216–225
29 Monte S. M. de la, Ganju N. and Wands J. R. (1999) Microtiter immunocytochemical ELISA assay: a novel and highly sensitive method of quantifying immunoreactivity. Biotechniques **26:** 1073–1076
30 Monte S. M. de la, Carlson R. I., Brown N. V. and Wands J. R. (1996) Profiles of neuronal thread protein expression in Alzheimer's disease. J. Neuropathol. Exp. Neurol. **55:** 1038–1050
31 Monte S. M. de la, Xu Y. Y. and Wands J. R. (1996) Modulation of neuronal thread protein expression with neuritic sprouting: relevance to Alzheimer's disease. J. Neurol. Sci. **138:** 26–35
32 Monte S. M. de la, Garner W. and Wands J. R. (1997) Neuronal thread protein gene modulation with cerebral infarction. J. Cereb. Blood Flow Metab. **17:** 623–635
33 Monte S. M. de la, Ghanbari K., Frey W. H., Beheshti I., Averback P., Hauser S. L. et al. (1997) Characterization of the AD7c-NTP cDNA expression in Alzheimer's disease and measurement of the 41-kD protein in cerebrospinal fluid. J. Clin. Invest. **100:** 1–12
34 Tortosa A., Lopez E. and Ferrer I. (1998) Bcl-2 and Bax protein expression in Alzheimer's disease. Acta Neuropathol (Berl) **95:** 407–412
35 MacGibbon G. A., Lawlor P. A., Sirimanne E. S., Walton M. R., Connor B., Young D. et al. (1997) Bax expression in mammalian neurons undergoing apoptosis, and in Alzheimer's disease hippocampus. Brain Res. **750:** 223–234
36 Kitamura Y., Shimohama S., Kamoshima W., Ota T., Matsuoka Y., Nomura Y. et al. (1998) Alteration of proteins regulating apoptosis, Bcl-2, Bcl-x, Bax, Bak, Bad, ICH-1 and CPP32, in Alzheimer's disease. Brain Res. **780:** 260–269
37 Desjardins P. and Ledoux S. (1998) Expression of ced-3 and ced-9 homologs in Alzheimer's s disease cerebral cortex. Neurosci. Lett. **244:** 69–72
38 Crawford D. R., Wang Y., Schools G. P., Kochheiser J. and Davies K. J. (1997) Down-regulation of mammalian mitochondrial RNAs during oxidative stress. Free Radical Biol. Med. **22:** 551–559
39 Crawford D. R., Abramova N. E. and Davies K. J. (1998) Oxidative stress causes a general, calcium-dependent degradation of mitochondrial polynucleotides. Free Radical Biol. Med. **25:** 1106–1111
40 Crawford D. R., Lauzon R. J., Wang Y., Mazurkiewicz J. E., Schools G. P. and Davies K. J. (1997) 16S mitochondrial ribosomal RNA degradation is associated with apoptosis. Free Radical Biol. Med. **22:** 1295–1300
41 Benowitz L. I. and Routtenberg A. (1997) GAP-43: an intrinsic determinant of neuronal development and plasticity. Trends Neurosci. **20:** 84–91
42 Monte S. M. de la, Federoff H. J., Ng S. C., Grabczyk E. and Fishman M. C. (1989) GAP-43 gene expression during development: persistence in a distinctive set of neurons in the mature central nervous system. Brain Res. Dev. Brain Res. **46:** 161–168
43 Masliah E., Hansen L., Albright T., Mallory M. and Terry R. D. (1991) Immunoelectron microscopic study of synaptic pathology in Alzheimer's disease. Acta Neuropathol (Berl) **81:** 428–433
44 Masliah E., Mallory M., Hansen L., Alford M., Albright T., DeTeresa R. et al. (1991) Patterns of aberrant sprouting in Alzheimer's disease. Neuron **6:** 729–739